ROTOR VIBRATION CAUSED BY EXTERNAL EXCITATION AND RUB

Osami Matsushita, Michiyuki Takagi, Katsuaki Kikuchi, and Makio Kaga
Mechanical Engineering Research Laboratory
Hitachi, Ltd.
502, Kandatsu-Machi Tsuchiura-shi,
Ibaraki-ken 300 Japan

SUMMARY

For turbomachinery with low natural frequencies, considerations have been recently required for rotor vibrations caused by external forces except unbalance one, such as foundation motion, seismic wave, rub and so forth. Such a forced vibration is investigated analytically and experimentally in the present paper.

Vibrations in a rotor-bearing system under a harmonic excitation are analyzed by the modal techique in the case of a linear system including gyroscopic effect. For a nonlinear system a new and powerful quasi-modal technique is developed and applied to the vibration caused by rub.

From the above analyses the following results are derived.

1. In a high speed rotor, two resonances of a forward whirl motion and backward one are induced under a directional external excitation, because of large gyroscopic effect. Although rub of rotor usually causes instability, it is possible to stabilize the rotor vibration by selecting a rubbing stopper suitable to each resonance severity.
2. In a low speed rotor such as a vertical pump with small gyroscopic effect, a response is a directional vibration within limits of no rubbing. However, when a rotor begins to rub, a directional respose changes to a stable forward whirl motion due to the nonlinearity in the water bearing.

These analytical results characterized by gyroscopic effect and bearing nonlinearity are confirmed by excitation tests of a high speed spin rotor and a pump model rotor, respectively.

1. INTRODUCTION

Many studies deal with vibration responses for some kinds of excitation in structure dynamics. However, a response of rotor under external excitation shows different features of motion from that of structure, i.e. forward whirl motion and backward whirl motion at each resonance. Some papers (ref. 1, 2) describe such a response of a rigid rotor.

In this paper, a general description of a forced vibration in linear rotor-bearing system is given and a rub vibration induced by contact between a rotor and a stator is also included in the discussion on nonlinear rotor dynamics.

Two kinds of rotors are selected for the study of rub vibration. The one is a rotor with high speed rotation and large gyroscopic effect. The stopper effect for the suppression of a rotor vibration due to rub is discussed. The other is a pump model rotor with low speed rotation and water lubricated bearings. Nonlinearity of a water bearing and rub vibration of a journal are considered.

SYMBOLS

B^*, B_i^* ; modal quantum in state equation
C_g ; gyroscopic matrix
C_g^* ; modal gyro
C_f, C_b ; complex type of damping matrix
C_{ij} (i,j = x,y) ; damping matrix
F ; external force
i ; imaginary unit $\sqrt{-1}$
I_d ; transverse moment of inertia of a disk
I_p ; polar moment of inertia of a disk
K_f, K_b ; complex type of stiffness matrix
K_{ij} (i,j = x,y) ; stiffness matrix
K ; stiffness of stopper with a clearance
K^* ; modal stiffness
m ; mass of a disk
M , M^* ; mass matrix , modal mass
S, S_i ; normal coordinate
t ; time
$Q_Z = Q_X + iQ_Y$; nonlinear restoring force
$Z = X + iY$; rotor absolute displacement
$z_O = x_O + iy_O$; foundation absolute displacement
$z = Z - z_O$; rotor relative displacement
δ ; clearance
$\zeta = -\alpha/|\lambda|$; modal damping ratio C/Cc
λ , λ_K ; complex eigenvalue
μ ; friction factor
ν ; excitation frequency
ϕ, ϕ_i ; eigen vector
ω , ω_f , ω_b ; natural frequency in rotation
ω_n ; natural frequency in no rotation
Ω ; rotational speed

2. EQUATION OF MOTION AND MODE SEPARATION

2.1 Equation of Motion in Rotor-Casing System

The equation of motion on a coordinate system fixed in the space is derived for entire system including a rotor, bearings and casing, as shown in Fig.1. The system is discretized by a beam model along longitudinal axis with ξ -direction. Representing the absolute displacements at each location of a rotor with X and Y and that of a casing with x and y , the equation of motion is given as follows

$$\begin{aligned} M\ddot{X} - \Omega C_g \dot{Y} + K_{xx}(X - x_o) + K_{xy}(Y - y_o) + C_{xx}(\dot{X} - \dot{x}_o) + C_{xy}(\dot{Y} - \dot{y}_o) &= Q_x \\ M\ddot{Y} + \Omega C_g \dot{X} + K_{yx}(X - x_o) + K_{yy}(Y - y_o) + C_{yx}(\dot{X} - \dot{x}_o) + C_{yy}(\dot{Y} - \dot{y}_o) &= Q_y \end{aligned} \qquad (1)$$

where Q_X and Q_Y are nonlinear restoring forces.

A complex numbered type of displacement is introduced here for the sake of convenience of description.

$$Z = X + iY \qquad z_O = x_O + iy_O \qquad (2)$$

Since the acceleration $\ddot{z}_O$ (t) of the foundation of the casing is usually measured, the equation (1) is rearranged to obtain the acceleration excitation of foundation. Applying relative displacement $z=Z-z_O$, where the rotor motion is measured with respect to the casing motion, the following equation of motion is obtained from Eq.(1).

$$M\ddot{Z} + i\Omega C_g \dot{Z} + K_f Z + K_b \bar{Z} + C_f \dot{Z} + C_b \dot{\bar{Z}} = -M\ddot{Z}_0 - i\Omega C_g \dot{Z}_0 + Q_Z \equiv F \qquad (3)$$

This formula is fundamental for the study of vibration under seismic excitation in rotor dynamics.

In the formula, the second term with the coefficient of rotational speed Ω shows gyroscopic effect which exists only in a rotor system. The matrices M and Cg consist of inertias of each disk on a shaft in the following forms.

$$\begin{aligned} M &\approx \text{diagonal}\ (\cdots m, I_d \cdots) \\ C_g &\approx \text{diagonal}\ (\cdots 0, I_p \cdots) \end{aligned} \qquad (4)$$

Therefore, if the casing moves in a parallel way with acceleration $\ddot{Z}_0 = [\ddot{\delta}_0, \ddot{\theta}_0 = 0]$, excitation force, stated on the righthand side of Eq.(3), reduces to only inertia force $M\ddot{Z}_0$ of mass as usual. On the other hand, if the casing is rocking in a non-parallel way with $\ddot{Z}_0 = [\ddot{\delta}_0, \ddot{\theta}_0]$, an additional force $-\Omega C_g \dot{\theta}_0$ adds up the excitation force. That is a gyroscopic moment which is proportional to a polar moment of inertia of disks and rotational speed.

2.2 Response at Each Mode

Table 1 is utilized to derive the modal response at each mode based upon orthogonality of eigensolution. There are two columns I and II in Tab.1. One of them concerns with a rotor system suspended vertically and the other one with a horizontally suspended rotor system. The former one indicates a free motion with a circular whirl and the latter one indicates a motion with an elliptical whirl. This classification is due to symmetry or asymmetry in bearing dynamic properties.

For each case, it is assumed that eigensolution of free equation of motion indicated in the line No.3 of table 1 is given by the formula as shown in the line No.4. The corresponding eigenvalue problem is obtained, and orthogonality condition is guaranteed in the forms given by the line No.8.

Therefore, by using these eigensolutions of free vibration, it is possible to separate a general response into each mode response on normal coordinate system. From a physical system with symmetrical bearings of I in Tab.1 to a normal coordinate system, the modal transformation is defined by the relationship as follows.

$$z = [\phi_1 \cdots\cdots \phi_m]s = [\Phi]\, s \qquad (5)$$

The state equation with normal coordinate resulted by post-transformation becomes

$$\dot{s}_i - \lambda s_i = -\frac{\lambda_i \phi_i^t F}{\beta_i^*} \qquad (6)$$

where $$\beta_i^* = -\lambda_i^2 \phi_i^t M \phi_i + \phi_i^t K \phi_i \rightarrow \beta^* = -\lambda^2 M^* + K^* \approx \omega^2 M^* + K^*$$

The normal transformation for a system with asymmetrical bearing of II in tab.1 is also derived by the same manner.

3. HARMONIC FOUNDATION EXCITATION

3.1 Harmonic Excitation

The external force in the equation of motion Eq.(3) becomes

$$F = -M\ddot{Z}_0 - i\Omega C_g \dot{Z}_0 \qquad (7)$$

where the harmonic acceleration in a certain direction e.g., fixed at X-axis

$$\ddot{z}_o = a \cos \nu t \qquad (8)$$

is substituted into Eq.(7). Then, the external force is defined as following exponential expression.

$$F = -\left(M + \frac{\Omega}{\nu} C_g\right) \frac{a}{2} e^{i\nu t} - \left(M - \frac{\Omega}{\nu} C_g\right) \frac{a}{2} e^{-i\nu t} \qquad (9)$$

Movements of the foundation in parallel and rocking motions are generally included in the amplitude a of an acceleration. As usual, in the case of no rocking motion the external force is simplified into the following formula.

$$F = -M \frac{a}{2} e^{i\nu t} - M \frac{a}{2} e^{-i\nu t} \qquad (9')$$

As the one directional force acts upon the rotor, it is equivalent to two whirling forces expressed by exponential form, with forward component $i\nu$ and backward component $-i\nu$.

Now, suppose that an eigenvalue $\lambda = -\alpha + i\omega \ (\omega > 0)$ with a rotor in rotation is obtained, a resonance occurs when excitation frequency ν comes close to a natural frequency ω i.e., $\nu \approx \omega$. On the other hand, the conjugate value $\bar{\lambda} = -\alpha - i\omega$ does not become an eigenvalue in rotor system, because of gyroscopic effect. So no resonance appears at the condition of $-\nu \approx -\omega$. Therefore, it is clear that only one of the two whirl forces contributes to a resonance.

Each whirl force, divided from one directional harmonic force, has half of the magnitude of one directional force. Then the rotor response on a resonance, while in rotation, is reduced to about half of the amplitude, compared with the one with no rotation.

3.2 Features of Response

Some features appearing in the response are summarized for a vertically suspended rotor here. A modal response corresponding to an eigenvalue and also to an eigen vector is obtained by substituting Eq.(9') into Eq.(6).

$$S(t) = \frac{\phi^t M}{\beta^*} \left\{ \frac{\lambda}{i\nu - \lambda} \frac{a}{2} e^{i\nu t} + \frac{\lambda}{-i\nu - \lambda} \frac{a}{2} e^{-i\nu t} \right\} \qquad (10)$$

[1] Forward Whirl Resonance; As the condition $\nu \to \omega_f$ with the relationship between eigenvalue $\lambda = -\alpha + i\omega_f$ and exciting frequency ν, a forward whirl resonance becomes remarkably large as described in the first part of Eq.(10).

$$S(t) \approx \frac{1}{2} \frac{\phi^t M}{K^*} \frac{2}{1 + \omega_f^2/\omega_n^2} \frac{a}{2\delta} e^{i(\nu t - 270°)} \qquad (11)$$

The phase relationship between rotor position and exponential exciting force is shown in Fig.3, for three instances of pre, on and post resonance when the excitation frequency is swept. The phase lag of rotor behind the force is 270 deg. when just on a resonance in the X-direction. And it is less than 270 deg. at pre-resonance and more than 270 deg. at post-resonance.

[2] Backward whirl Resonance; When the relationship between eigenvalue $\lambda = -\alpha - i\omega_b$ and excitation frequency ν approaches the range of $-\nu \approx -\omega_b$, the rotor response becomes a backward resonance, as described in the second part of Eq.(10).

$$S(t) \approx \frac{1}{2} \frac{\phi^t M}{K^*} \frac{2}{1 + \omega_b^2/\omega_n^2} \frac{a}{2\delta} e^{-i(\nu t - 270°)} \qquad (12)$$

The phase lag of rotor behind the force is 270 deg. when just on a resonance. And it is changing from less than 270 deg. to more than 270 deg. through the resonance as shown in Fig.4.

[3] Whirl Motion; The rotor has two eigenvalues which correspond to a mode shape. These values are different from conjugate relation and are independent from each other. Here the forward natural frequency is higher than the backward one.

Therefore, when rotating the rotor at a high speed, the response whirl motion is changing from left to right as shown in Fig.5, corresponding with increase of excitation frequency. At the beginning the backward resonance occurs with a circular orbit, and later on through elliptical orbits the forward resonance appears again with a circular whirl orbit. On the boundary line, between forward direction and backward direction, an elliptical whirl orbit becomes a straight line thus whirl direction can be interchanged.

[4] Low Gyroscopic Effect; In the case of low gyroscopic effect such as low rotational speed or small disks, forward eigenvalue and backward one corresponding to an eigen mode are not independent of each other, and they approach to a conjugate relation. The typical state such as low gyroscopic effect leads to dynamics of nonrotational rotor. Eigenvalues maintain conjugate form, for example,

$\lambda_K = \lambda \qquad \lambda_{K+1} = \bar{\lambda}$

Resonance response is described by the following form

$$S(t) \approx \frac{1}{2} \frac{\phi^t M}{K^*} \left\{ -\frac{\lambda}{i\nu - \lambda} e^{i\nu t} + \frac{\bar{\lambda}}{-i\nu - \bar{\lambda}} e^{-i\nu t} \right\} \qquad (13)$$

such that rotor, vibrating only in X-direction, coincides with the direction of the acting force without a whirl motion.

3.3 Harmonic Respose Curve

Figure 8 shows the response curve under harmonic excitation. In the case of $\Omega = 0$ i.e., no rotation, a resonance peak appears. On the other hand, at high speed rotation two resonance peaks appear with backward whirl and forward whirl. The separation of a peak into two peaks is due to gyroscopic effect or rotor rotation. This figure is described by nondimensional frequency and amplitude, which are normalized by the values of the resonance frequency and amplitude at no rotation, respectively. The peak at the forward resonance is less than the half of the peak at the resonance in no rotation, because of $\omega_f / \omega_n \geq 1$ in Eq. (11). On the other hand, the peak at the backward is more than the half of that, because of $\omega_b^2 / \omega_n^2 \leq 1$ in Eq. (12). Therefore it is clear that these two peak amplitudes reduce to about half of the amplitude at no rotation and the backward amplitude is slightly higher than the forward one.

4. SEISMIC EXCITATION

Instead of equation of motion in physical coordinate system, the state equation in normal coordinate system is used for analysis of time history response caused by seismic excitation. In Eq.(6), an arbitrary external force

$$F = -M\ddot{z}_0 - i\Omega C_g \dot{z}_0 \qquad (14)$$

is defined by insertion of the acceleration $\ddot{z}_0$ measured in the field. Substitution of Eq.(14) into Eq.(6) and integration of the resulting equation gives time history response of rotor in normal coordinate system. In order to return the normal response to the response in physical system the following relationship is used:

$$z(t) = \sum_i \phi_i S_i(t) \qquad (15)$$

5. SEISMIC EXCITATION WITH NONLINEAR SYSTEM

Here we discuss a rotor vibration induced by seismic excitation which becomes larger than the clearance between a rotor and a stopper. In such situation the rotor begins to contact the stopper fixed on the casing.

In this rub vibration, the response on normal coordinate system is given by Eq.(6) and the external force is defined as follows.

$$F = -M\ddot{z}_o - i\Omega C_g \dot{z}_o + Q_z \qquad (16)$$

The force Qz is a nonlinear restoring force generated by the contact of a rotor with a stopper. The two types of configuration of a cylindrical stopper are mentioned here.

(1) Type I contact between an outer surface of a rotor and an inner surface of a stopper i.e., a rotor in a stopper

(2) Type II contact between an inner surface of a rotor and an outer surface of a stopper i.e., a stopper in a rotor

The types I and II here are called an outer contact and an inner contact with respect to the rotor.

Representing the stiffness of a stopper, the clearance between a rotor and a stopper and the friction factor with K, δ and μ, respectively, the nonlinear restoring force is defined as follows.

$$Q_z = F_r \pm i F_\theta \qquad \begin{matrix} + \text{ for outer contact type} \\ - \text{ for inner contact type} \end{matrix} \qquad (17)$$

where $$F_r = -K(|z| - \delta) z/|z|$$

and $F_\theta = \mu F_r$ sign (angular velocity of contact face on rotor)

In the simulation of a nonlinear vibration caused by rub, the second term in Eq.(17) indicates an unstable friction force which induces a whirl motion. Therefore, to suppress the rotor vibration by a cylindrical stopper, the outer type of a stopper is more effective in a rotor with higher forward resonance severity. On the other hand, the inner type of a stopper is more effective with higher backward resonance severity.

For the response history analysis in such a nonlinear system a quasi-modal technique is effective, and a hybrid integration method based upon it is developed, as described in Appendix.

6. EXCITATION TEST OF HIGH SPEED ROTOR

6.1 Harmonic Excitation

The features of a rotor response excited by a harmonic wave, stated in the previous chapters, are reconfirmed by an experiment in which the rotor shown in Fig.7 is used. The rotor rotates in very high speed, and it has large gyroscopic effect. The rotor is suspended by bearings at both sides. The vibration mode with a low natural frequency is the conical mode in which the right side of the rotor vibrates with the nodal point in the left side.

The vibration response waveform, the response curve and the Lissajous figure of rotor motion are presented in Fig.8, including a harmonic waveform with the excitation frequency ν. When the rotor does not rotate, the rotor vibration response is one directional and the resonance frequency agree with the natural frequency ω_n in a structure i.e., $\nu = \omega_n = 4.95$ Hz.

Under a rotation of the rotor, two resonance peaks in the rotor response appear in the backward and forward resonances at the excitation frequency $\nu = 0.66\omega_n$ and $\nu = 1.21\omega_n$, respectively. The peak amplitude severity Q at the backward resonance becomes about half of the peak amplitude severity $Q_n = 156\ \mu m/gal$ at the resonance of the rotor with no rotation. The other one at the forward resonance is about one fifth of Q_n. The calculated values of the resonance frequency and peak amplitude severity, as shown in Fig.5, well coincide with these experimental values.

6.2 Rub Vibration

An aseismic stopper with a fine gap is installed in the rotor system with large gyroscopic effect, as schematically shown in Fig.7. This stopper is not a usual circular type, but one directional type with a clearance of x-direction as shown in (i) of Fig.6.

Figure 9 shows vibration history response and its Lissajous figure of the rotor subjected to a seismic wave. The magnitude of excitation acceleration increases in turn by (A), (B) and (C). In the case of (A), excitation acceleration is so small that the rotor moves in the clearance with no rub and nearly circular whirl orbit. In the case of (B) and (C) rubs occur. Comparing the case (C) with the case (B) a larger acceleration causes a stronger rub between the rotor and the stopper, close to an impact.

In the rotor system with large gyroscopic effect, the vibration of a rotor is always generated in a circular whirl motion by an external force in one direction. Then, vibration is satisfactorily suppressed by even one directional stopper at an arbitrary phase location, as demonstrated in this numerical simulation. One directional stopper is rather preferable than a circular stopper, because the duration of rub in the former is less than one in the latter and the corresponding friction force which induces unstable vibration becomes less.

The effect of the stopper upon vibration suppression is indicated in Fig.10. The horizontal axis shows the maximum value of the acceleration in the seismic wave, normalized by the value in which the rotor begins to rub with the stopper. The perpendicular axis gives the value of the displacement in the response, normalized by the clearance δ. The stable suppression of the rotor vibration is seen in the range of about five times of the acceleration at the beginning of rub in Fig. 10. This numerical result proves a good agreement with the corresponding experimental result.

7. EXCITATION TEST OF PUMP MODEL ROTOR

7.1 Outline of Experiment

Figure 11 shows the outline of the experimental equipment which is simplified into a vertically suspended pump model rotor for atomic power plant. The experimertal rotor has two disks and two bearings. A self-centering ball bearing is used at the upper part and water is filled in the cylindrical water bearing located at the lower part. Two weights are added to the lower part of the rotor. An aseismic support is located at the lowest part of the casing in order to prevent large vibration of the casing.

The pump model rotor is vertically located on a shaking table which can stand the load of 294 kN (30 tons). The excitation wave is sinusoidal one in this test. In this measurement system, the usual way is employed, except for a load cell with strain gages to measure the dynamic force in the lower water bearing.

7.2 Natural Frequency

The experimental rotor is discretized by beam element and a calculation model is obtained as shown in Fig.11. Natural frequencies and corresponding mode shapes are represented in Tab.2 and Fig.12,respectively.

From the calculation results considering virtual mass effect (Ref.3) of water and assuming water bearing stiffness of 9.8 MN/m (10^3 kgf/mm) natural frequencies are 13.6 Hz and 18.0 Hz. With the stiffness of 39.2 kN/m (4.0 kgf/mm), they are 14.9 Hz, 6.4 Hz and 27.6 Hz. The former stiffness is picked up to simulate the contact of the journal with the stator of bearing under the condition of large journal vibration, and the latter one is equivalent to the stiffness of water bearing under the condition of small journal vibration. In the latter, the rotor vibrates remarkably in the first and second mode and the casing in the first mode.

The comparison of calculation values of natural frequency with experimental ones is presented in Tab.2. The first natural frequency of 6.4 Hz in calculation agrees well with the experimental value of 7.0Hz. Concerning the casing mode, a good agreement is also obtained by comparison between the calculation value of 13.6 ~ 14.9 Hz and the experimental value of 14.0 Hz.

With respect to the second natural frequency of rotor mode, the experimental value of 18 ~ 20 Hz is negligibly different from the calculation value of 27.6 Hz under the assumption of no contact within small journal vibration. However, in the case of large stiffness i.e., assuming a contact in the bearing, this experimental value becomes close to the value obtained by the calculation. From these comparisons, it is estimated that the restoring force with a hard type of nonlinearity due to a contact is induced in a water lubricated bearing, and the large journal vibration increases the bearing stiffness.

The first mode resonance does not appear remarkably in the excitation test because of very high modal damping ratio.

As stated above, the good agreement of natural frequencies between the calculation and the experiment suggests the reasonable modeling of the pump rotor system, including dynamics in the water bearing.

7.3 Rotation Test

A rotation test is done before an excitation test. In this test the casing is tightly fixed by the aseismic support with no clearance. The vibration of the rotor itself is seen in the amplitude response curve in Fig.13. The first unbalance resonance appears at the rotational speed of 7 ~ 8 rps.

The second resonance varies greatly with the unbalance. In the case of a small unbalance, the second resonance peaks occur at the rotational speed of 17 ~ 19 rps. It changes to 20 rps when a large unbalance is applied to the rotor. It is noticed that the peak amplitude becomes very sharp in this case.

The large unbalance induces a large amplitude of vibration such that the rotor moves in a large whirl orbit in the clearance of the bearing, and the rub often occurs. Consequently the increase of the stiffness and the decrease of the damping effect at the bearing are induced by a large whirl motion and they lead to a sharper amplitude and a higher resonance frequency. In fact the scratches of rub can be seen when opening the bearing.

The comparison between amplitude responses in the rotation test and in the harmonic excitation test with no rotation is described in Fig.13 and 14. Both response curves are very different from each other. In the excitation test, only one high peak appears at the excitation frequency of about 18 Hz. Its response curve is similar to the unbalance response curve with large unbalance.

Therefore, it can be said that this excitation acceleration of 0.1 G seems to be small in value, but it has a large influence on the rotor vibration. From the fact, an actual pump rotor with low load capacity in the water bearing is very sensitive to an external excitation. This fact indicates the necessity of aseimic design for a pump rotor suspended vertically.

7.4 Harmonic Excitation Test

Influence of some parameters on a rotor response is examined by sweeping of a harmonic excitation frequency.

(1) Influence of Clearance in Water Bearing

The displacement of the rotor vibration is shown in Fig.14 by changing the bearing clearance of 0.127 mm and 0.381 mm. Here, the casing is fixed by the aseismic stopper with no clearance. In case of 0.127 mm (normal specification), the resonance occurs at the excitation frequency of 18.5 Hz and its peak amplitude reaches up to the value of 760 μm. With the clearance of 0.381 mm, the corresponding peak amplitude is 580 μm. As shown in the response curve with the clearance of 0.381 mm, larger clearance results in high damping effect which reduces the peak amplitude, and it produces a curve which shows true nonlinear phenomena due to a hard spring.

(2) Influence of Rotor Rotation with Fixed Casing

A harmonic excitation test is done at each rotational speed with the casing being fixed. The rotor response and dynamic bearing load, including the responses in X and Y direction, are summarized in Figs.15.

When the rotor is rotating and is subjected to harmonic excitation, Y-direction vibration appears in addition to X-directional vibration. This result indicates that a rotor response is a whirl motion, in spite of the extremely small gyroscopic effect in the pump rotor against the fact as mentioned in paragraph 3.2. It is seen that the hydraulic force in a fine clearance and the rub force due to larger journal vibration cause a whirling agitation for a rotor.

From these graphs, it is clear that an increase in rotational speed decreases the response peak amplitude and the dynamic bearing load in X-direction. However, the peak amplitude and the bearing load increase in Y-direction. When a rotor is in rotation, the sum of vibration responses in both directions becomes in balance with the power of external force. Then, it is clear that a rotor with no rotation is most sensitive to an external force and the rotation reduces such sensitivity.

Although two peaks are seen in a response curve just like influence of gyroscopic effect, it is not clear why the separation of a peak appears in spite of the rotor with an extremely small gyroscopic effect.

7.5 Whirl Orbit due to Rub

The response waveforms and whirl orbits of the journal motion at a resonance in the sweeping test are given in Fig.16. The one directional orbit at the no rotation changes into a circular whirl orbit with rotation due to rub. Therefore, the waveform of the bearing load at the rotation contains the ordinary harmonic component plus the spiky peak component due to rub.

7.6 Simulation of Rub Vibration

A dynamic model of the water bearing is assumed by a nonlinear relationship between the journal of displacement and the restoring force, as described in Fig.17. The nonlinear stiffness K is extremely greater than the linear stiffness K_o, like a hard type of spring.

The numerical result given in Fig.18 simulates a resonance in the harmonic sweeping test. The journal vibration is suppressed by the bearing clearance, but the Y-directional vibration occurs simultaneously near the resonance. The waveform of the bearing load is nearly harmonic. High spiky peak is superposed on the harmonic one at the instance of rub, like projections on the waveform of bearing load.

The whirl orbits obtained in the calculation of history response are shown in Fig.19. At no rotation of 0 rps, one directional vibration is generated, coinciding with the excitation direction. A whirl motion is induced by rub at the rotation of 24 rps.

Comparing Fig.19 with Fig.16, the calculated whirl orbit at no rotation agrees with the experimental one. With respect to results at 24 rps, they are different from each other. The experimental whirl orbit is nearly circular and the calculation one closes to be rectangular. The disagreement may be attributed to the fact that a whirling force, generated in a fine gap when the journal rubs with the stator in the water bearing, and an unbalance force which actually exists are neglected in the calculation.

The comparison of the bearing load between the experiment and calculation is given in Fig.20. The horizontal axis shows the value assumed by a nonlinear stiffness K. Generally speaking, good agreement is seen with respect to the harmonic component and the spiky peak component in the bearing load waveform.

8. CONCLUSIONS

Conclusions summarized in this study are as follows.

(1) The modal technique is acceptable for the vibration analysis in a linear system with rotor, casing and bearings under an external excitation, and the division of the vibration response at harmonic excitation into each component of eigen modes is achieved. On the other hand, for the nonlinear vibration analysis, a new technique called quasi-modal is developed, and a hybrid integration method based on it is presented. The effectiveness of the new method is proved by numerical simulations of vibration due to such rub and nonlinearity in a water bearing.

(2) The peak amplitudes at a backward resonance and a forward resonance under a harmonic excitation when rotating a rotor in high speed are reduced to about half of the peak amplitude at no rotation. It is also proved that the backward resonance severity is slightly greater than the forward one. These general features of rotor response at a harmonic excitation are made clear in relation to gyroscopic effect.

(3) The selection of a stopper for the suppression of rotor vibration i.e., inner or outer type, depends upon which response severity is greater between a backward resonance and a forward one. It is verified by calculation and experiment that one directional stopper is rather stable and effective for the suppression of rotor vibration in the system with large gyroscopic effect, compared with a cylindrical type of stopper as usually used.

(4) Very high response sensitivity of vertically suspended rotor such as a pump to external excitation and rub becomes experimentally clear, including the dependence on bearing clearance and rotational speed.

(5) In spite of very small gyroscopic effect in a pump rotor, the rotor response indicates a whirl motion due to rub and nonlinearity in a water bearing. The response of bearing dynamic load contains a ordinary harmonic component and a spiky component in waveforms. It is demonstrated that these experimental values of bearing load can be estimated by the calculation assuming a dynamic model of a water bearing with clearance.

REFERENCES

(1) Kawamoto, I and Urushidani, H ; Trans. JSME, vol.45-400 (1979-12), P 1451
(2) Kanai, S. and Tamura, A. ; Preprint, JSME No 784-5 (1978-3), P 77
(3) Fritz, R.J. ; Trans. ASME Ser. B, 94-2 (1972-2), P 167

TABLE 1. - DAMPED EIGENVALUE ANALYSIS OF ROTOR-BEARING SYSTEM

No.	ITEM	I	II
1	SYSTEM	Circular Whirl Orbit with Symmetric Support Vertically Suspended Rotor	Eliptical Whirl Orbit with Asymmetric Support Horizontally Suspended Rotor
2	DYNAMIC PROPERTIES OF BEARING	$k_{xx}=k_{yy}\quad k_{xy}=-k_{yx}$ $c_{xx}=c_{yy}\quad c_{xy}=-c_{yx}$	——
3	EQUATION OF MOTION	$M\ddot{z}+i\Omega C_g\dot{z}+(C_d-iC_c)\dot{z}+(K_d-iK_c)z=F$	$M\ddot{z}+i\Omega C_g\dot{z}+C_t\dot{z}+C_b\dot{z}+K_tz+K_bz=F$
		where $K_t=K_d-iK_c=\left[\frac{k_{xx}+k_{yy}}{2}\right]+i\left[\frac{k_{yx}-k_{xy}}{2}\right]$ $C_t=C_d-iC_c=\left[\frac{c_{xx}+c_{yy}}{2}\right]+i\left[\frac{c_{yx}-c_{xy}}{2}\right]$	$K_b=\left[\frac{k_{xx}-k_{yy}}{2}\right]+i\left[\frac{k_{yx}+k_{xy}}{2}\right]$ $C_b=\left[\frac{c_{xx}-c_{yy}}{2}\right]+i\left[\frac{c_{yx}+c_{xy}}{2}\right]$
4	EIGEN SOLUTION	$z=\phi e^{\lambda t}$	$z=\phi_t e^{\lambda t}+\bar{\phi}_s e^{\bar{\lambda} t}\qquad \lvert\phi_t\rvert > \lvert\phi_s\rvert$
5	EIGENVALUE PROBLEM $\lambda B\Phi=A\Phi$ cf. $\lambda B^{-1}\Psi=A^{-1}\Psi$	$B=\begin{bmatrix}-M & 0\\ 0 & K_d-iK_c\end{bmatrix}\qquad \Phi=\begin{bmatrix}\phi\lambda\\ \phi\end{bmatrix}$ $A=\begin{bmatrix}i\Omega C_g+C_d-iC_c & K_d-iK_c\\ K_d-iK_c & 0\end{bmatrix}$	$B=\begin{bmatrix}B_1 & B_2\\ \bar{B}_2 & \bar{B}_1\end{bmatrix}\ B_1=\begin{bmatrix}-M & 0\\ 0 & K_t\end{bmatrix}\ B_2=\begin{bmatrix}0 & 0\\ 0 & K_b\end{bmatrix}\ \Phi=\begin{bmatrix}\phi_t\lambda\\ \phi_t\\ \phi_s\bar{\lambda}\\ \phi_s\end{bmatrix}$ $A=\begin{bmatrix}A_1 & A_2\\ \bar{A}_2 & \bar{A}_1\end{bmatrix}\ A_1=\begin{bmatrix}i\Omega C_g+C_t & K_t\\ K_t & 0\end{bmatrix}\ A_2=\begin{bmatrix}C_b & K_b\\ K_b & 0\end{bmatrix}$
6	MATRIX B, A	symmetric	——
7	EIGENVALUE	$\lambda=\alpha+iq$ Damped Frequency $=q$	Modal Damping $=-\alpha/\sqrt{\alpha^2+q^2}$
8	ORTHOGONALITY CONDITION	$\Phi_i^t B\,\Phi_j\begin{cases}=0\\ \neq 0\end{cases}\quad \Phi_i^t A\,\Phi_j\begin{cases}=0\\ \neq 0\end{cases}\quad \begin{matrix}\text{for } i\neq j\\ \text{for } i=j\end{matrix}$	$\Psi_i^t B\,\Phi_j\begin{cases}=0\\ \neq 0\end{cases}\quad \Psi_i^t A\,\Phi_j\begin{cases}=0\\ \neq 0\end{cases}\quad \begin{matrix}\text{for } i\neq j\\ \text{for } i=j\end{matrix}$
9	FORCED VIBRATION	$B^*(s-[\lambda]s)=[\lambda]Mod(\phi)\cdot F$ where $z=\sum\phi_i s_i \quad \text{for } i=1\sim 2n$ $=Mod(\phi)\cdot s$	$B^*(s-[\lambda]s)=[\lambda](Mod(\psi_i^t)\cdot F+Mod(\bar{\psi}_i^t)\cdot\bar{F})$ where $z=\sum(\phi_t s_i+\bar{\phi}_s\bar{s}_i) \quad \text{for } i=1\sim 2n$ $=Mod(\phi_t)\cdot s+Mod(\bar{\phi}_s)\cdot\bar{s}$

TABLE 2. - COMPARISON OF NATURAL FREQUENCIES

Item	Vibration Mode			Comment
	CASING	ROTOR		
	1-ST	1-ST	2-ND	
	Natural Frequency, Hz			
EXPERIMENT				
Impulse response	14.0			Hit casing
Unbalance response	14.0	7	17-19	
Harmonic excitation	14.0	No peak	18-20	Rotation N = 20 rps
CALCULATION				
Water bearing (linear)	14.9	6.4	27.6	Bearing stiffness = 4.0 kgf/mm = 39 kN/m (no rub)
Water bearing (nonlinear)	13.6		18.0	Bearing stiffness = 10^3 kgf/mm = 9.8 MN/m (with rub)

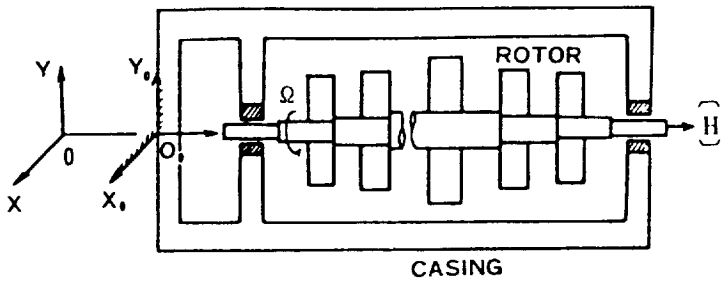

Figure 1. - Rotor-bearing-casing system.

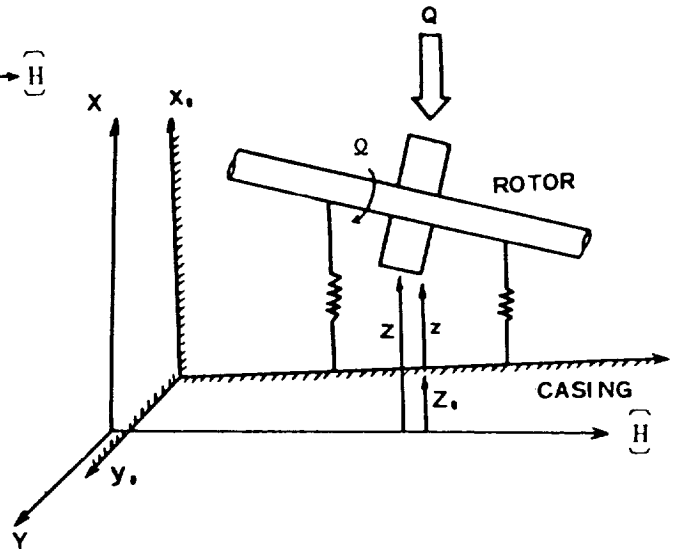

Figure 2. - Coordinate system.

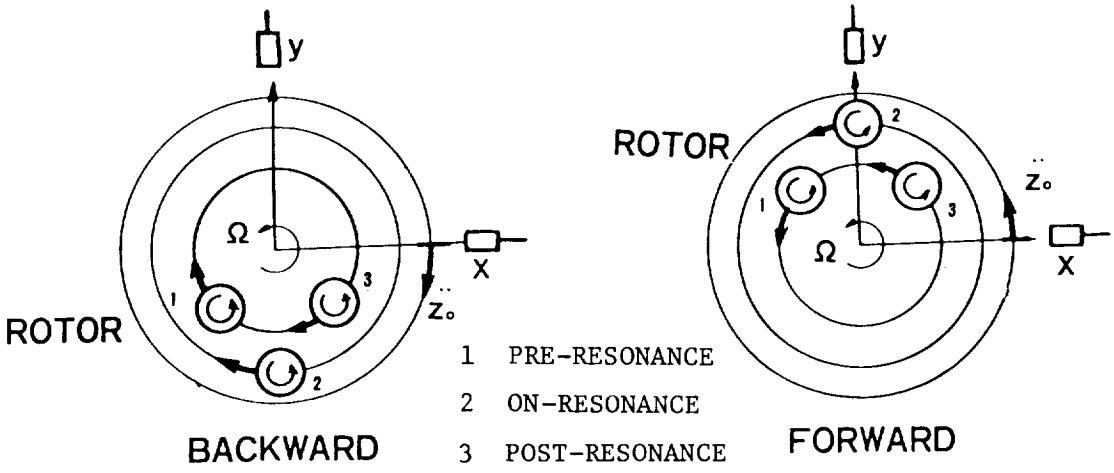

Figure 3. - Phase relationship between rotor and excitation acceleration.

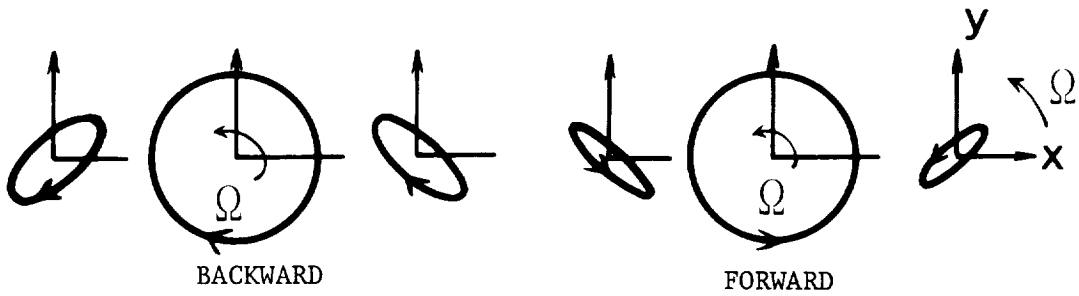

Figure 4. - Whirl orbit.

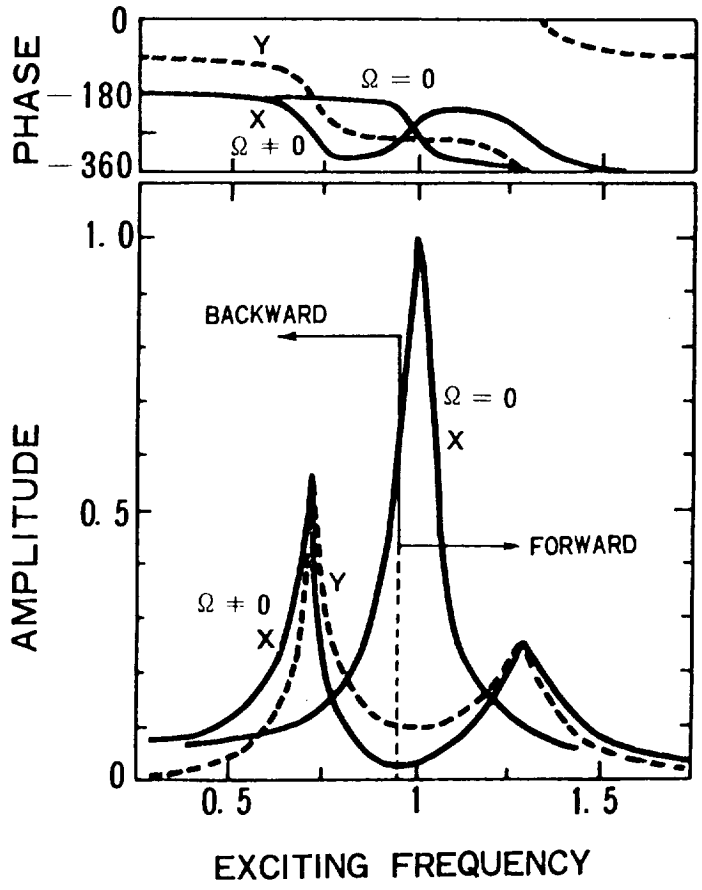

Figure 5. - Response curve in harmonic excitation.

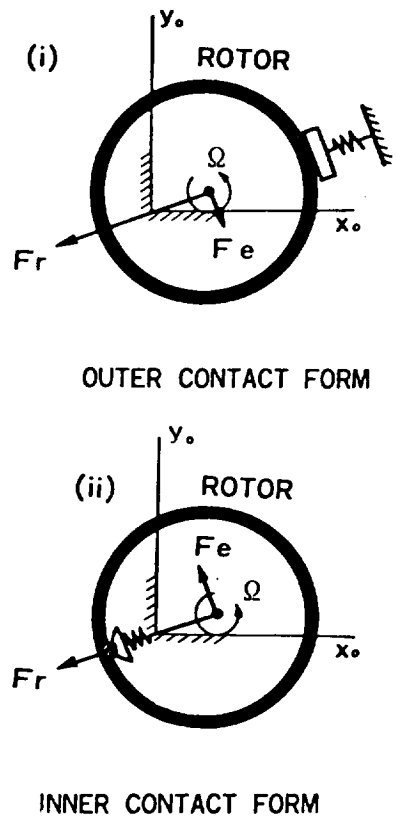

Figure 6. - Stopper with clearance.

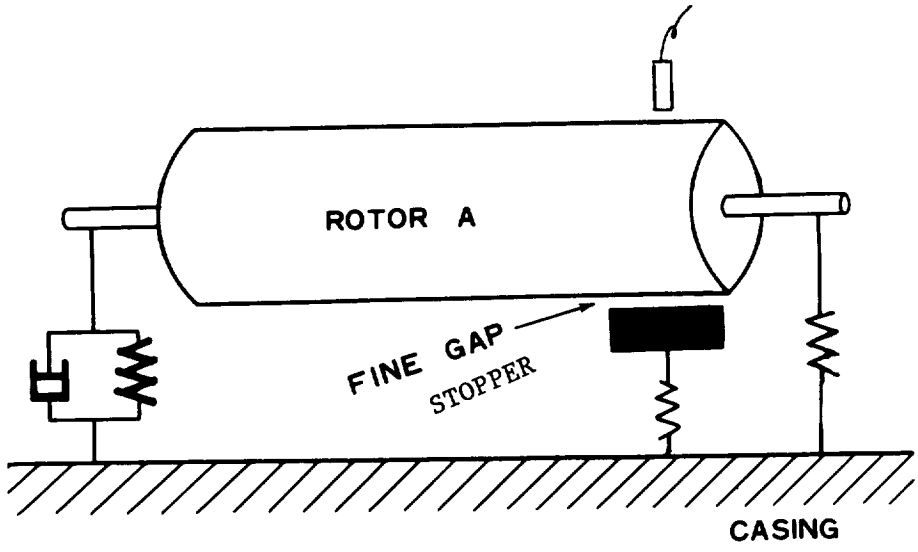

Figure 7. - A high speed rotor.

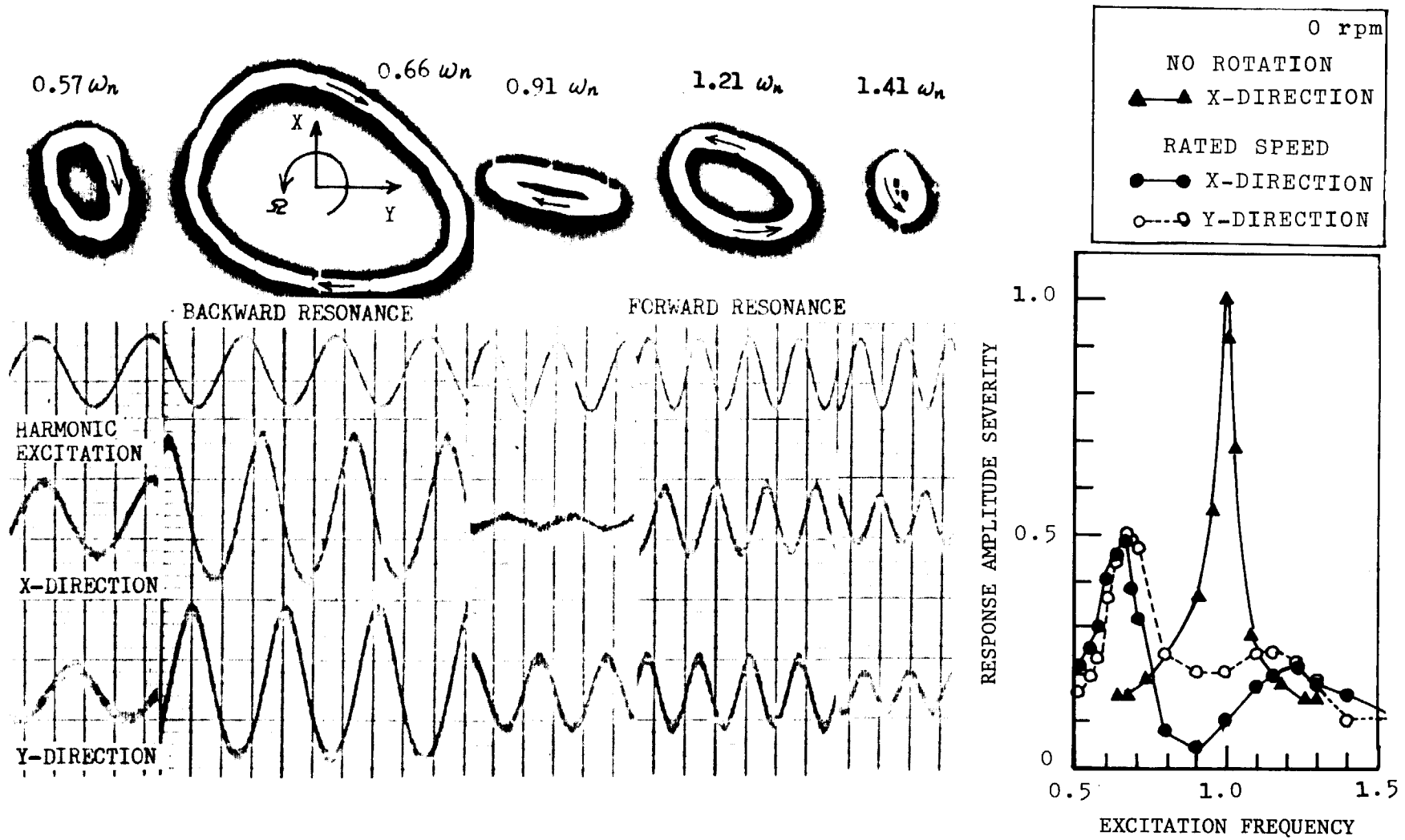

Figure 8. - Response of high speed rotor in harmonic excitation.

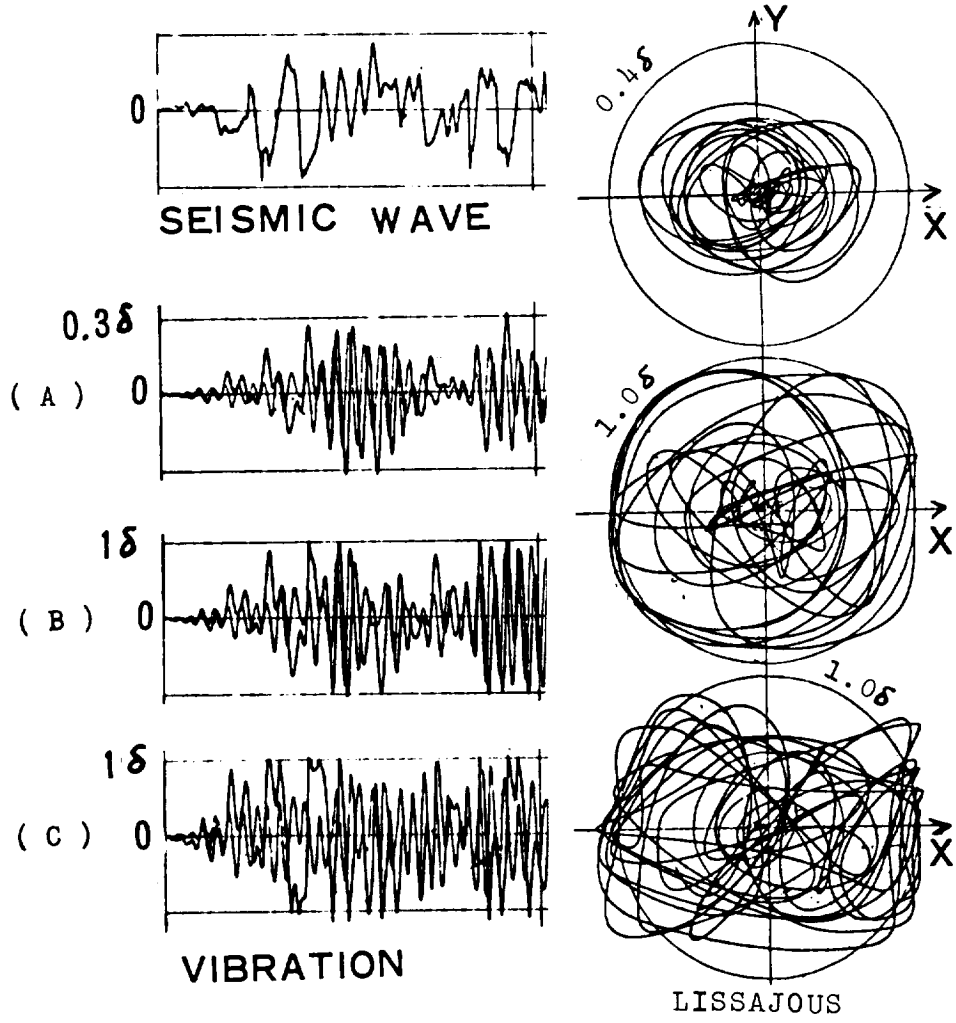

Figure 9. - History response analysis (one directional stopper).

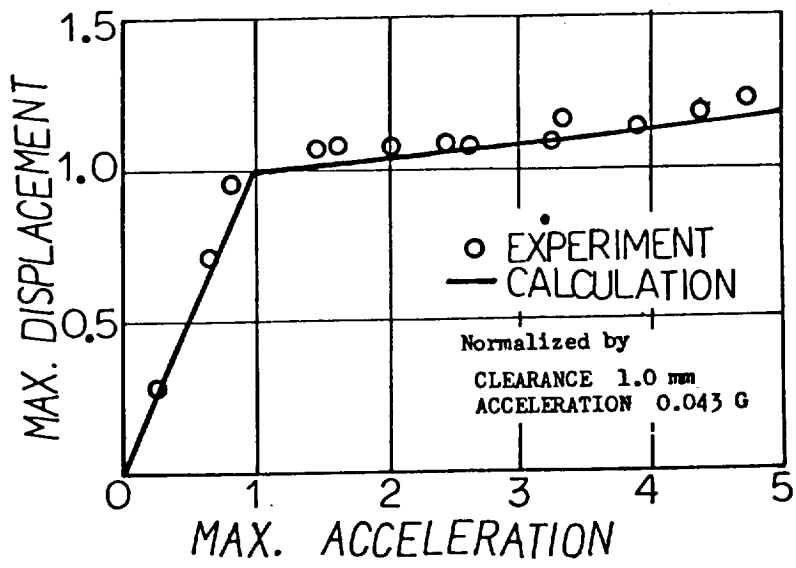

Figure 10. - Suppression of rotor vibration by stopper.

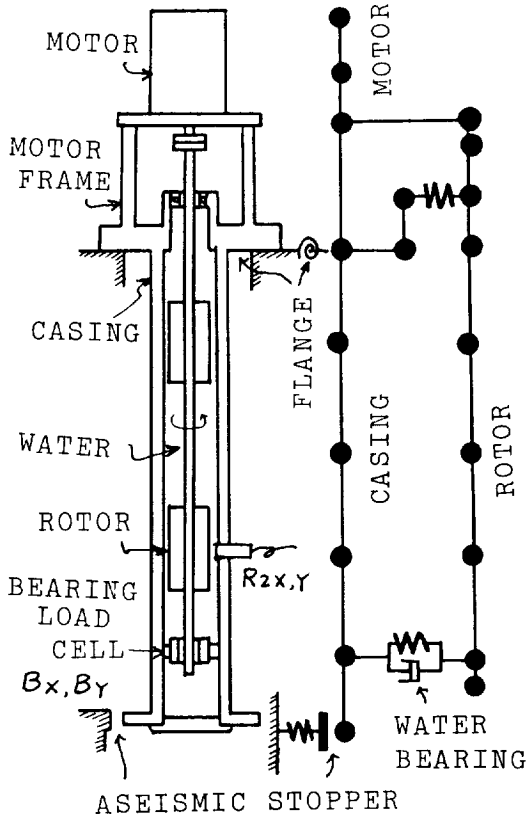

Figure 11. - A pump model rotor and its beam model.

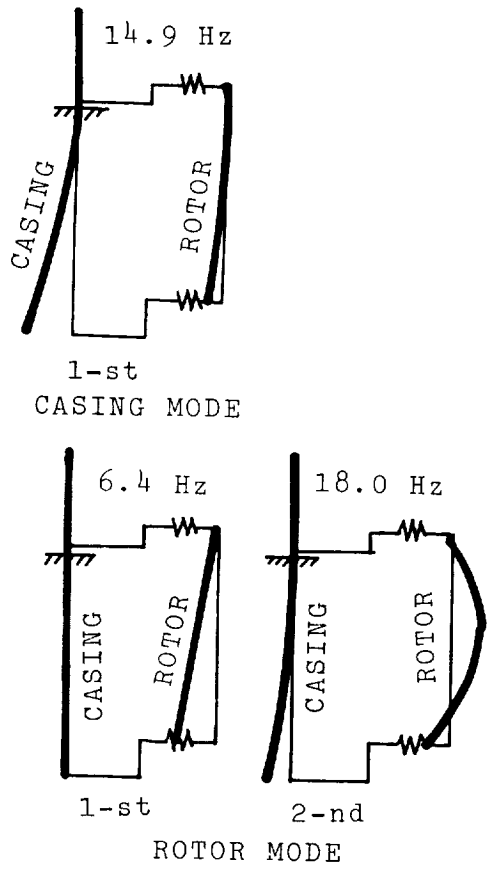

Figure 12. - Free eigen modes.

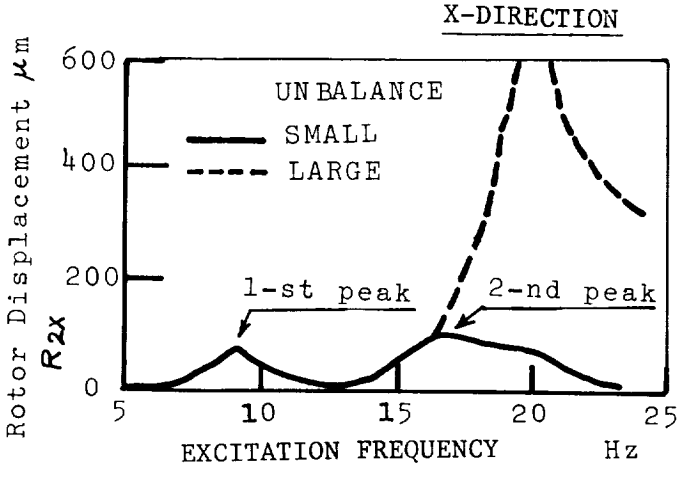

Figure 13. - Influence of unbalance.

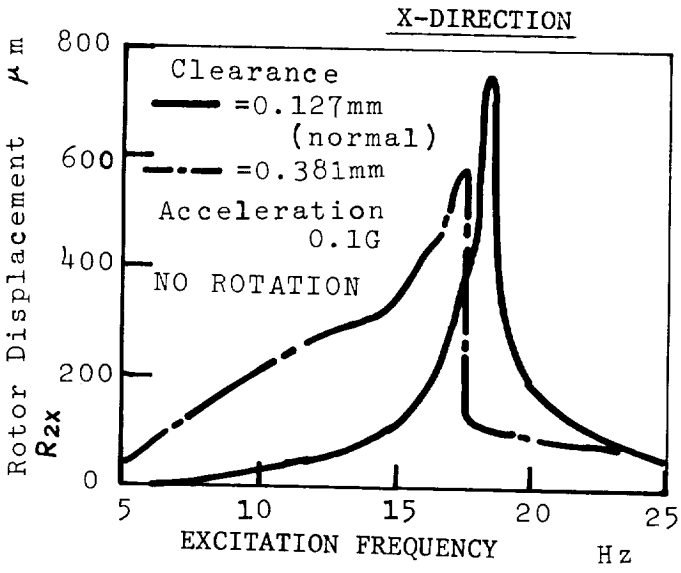

Figure 14. - Influence of clearance in water bearing.

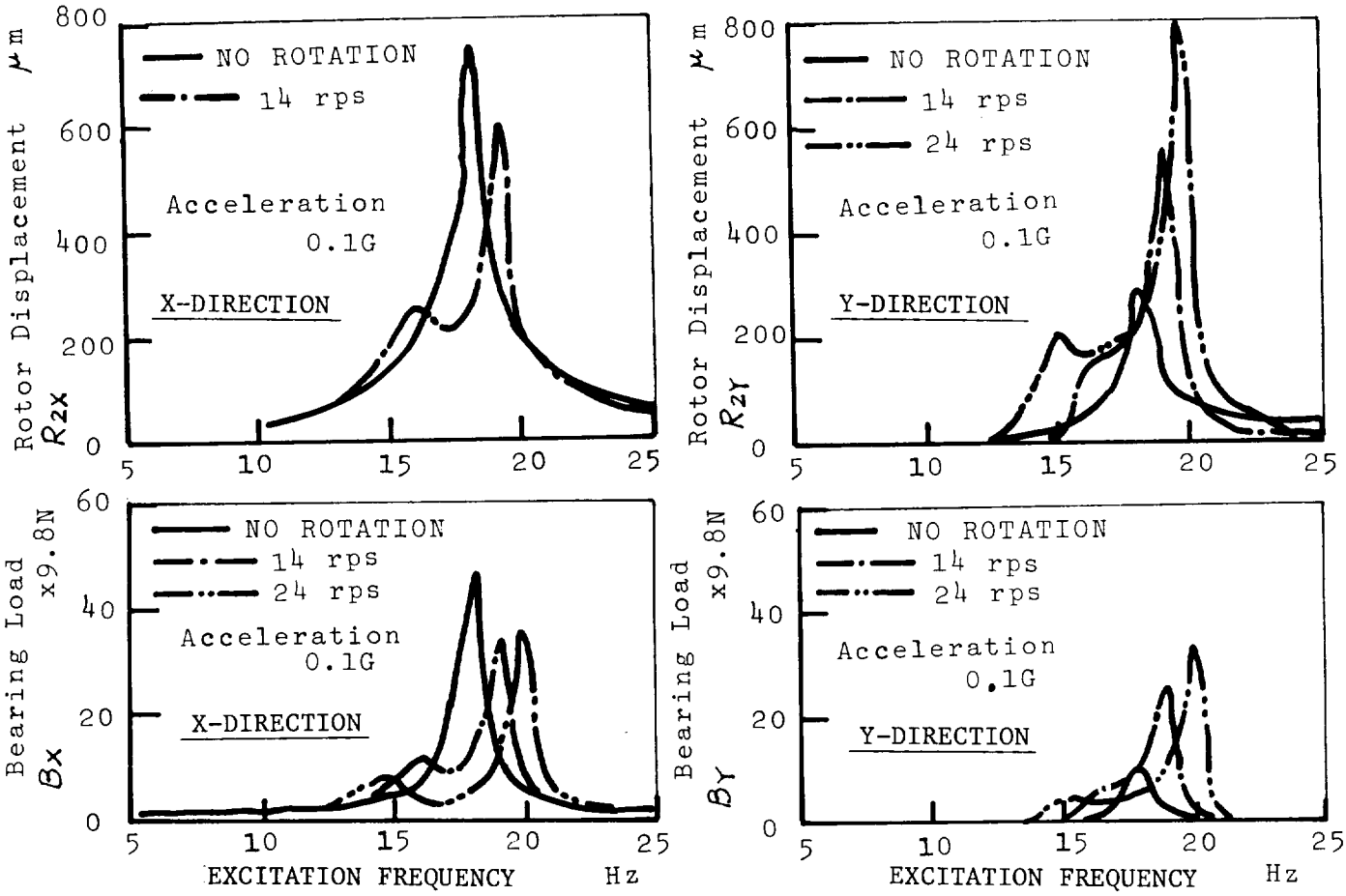

Figure 15. - Influence of rotational speed.

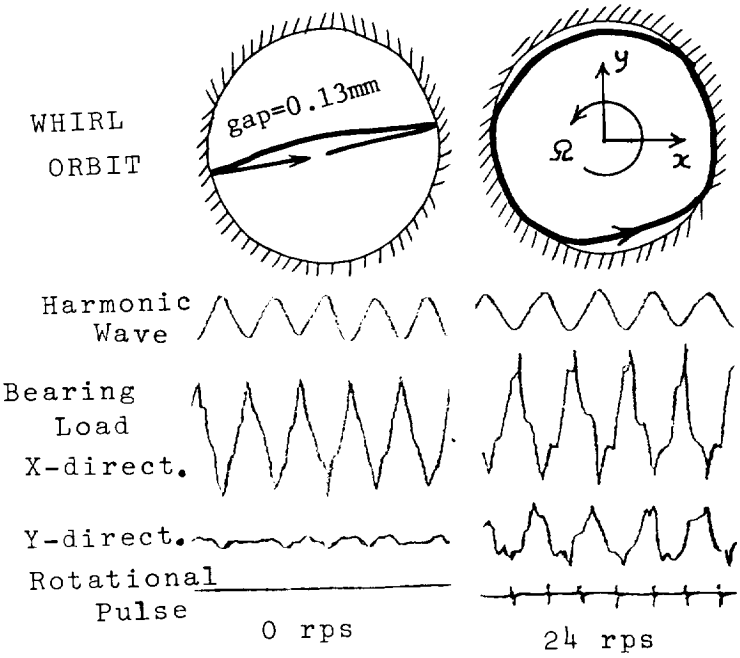

Figure 16. - Waveforms and whirl orbits.

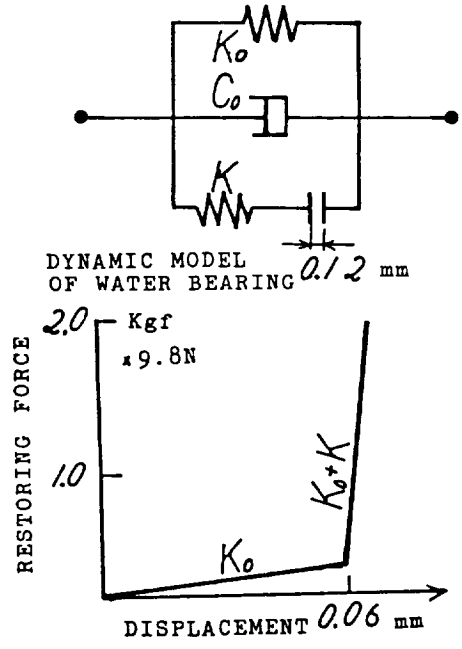

Figure 17. - Restoring force in water bearing.

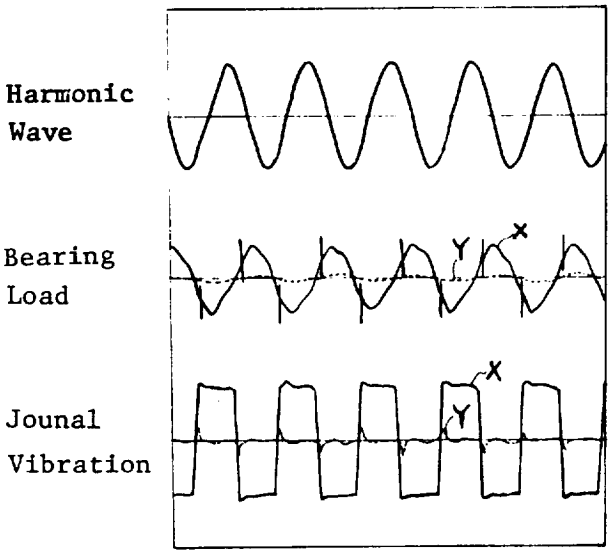

Figure 18. - Response waveforms near a resonance.

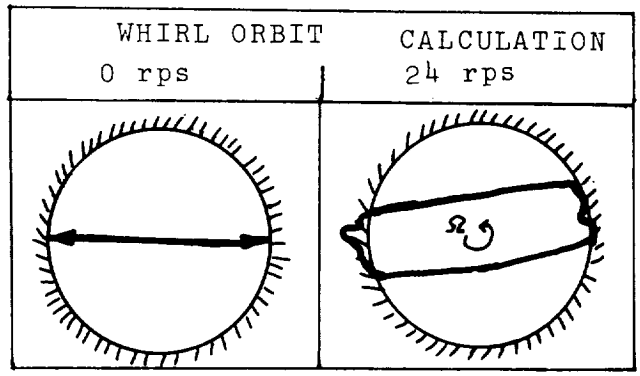

Figure 19. - Whirl orbit in resonances.

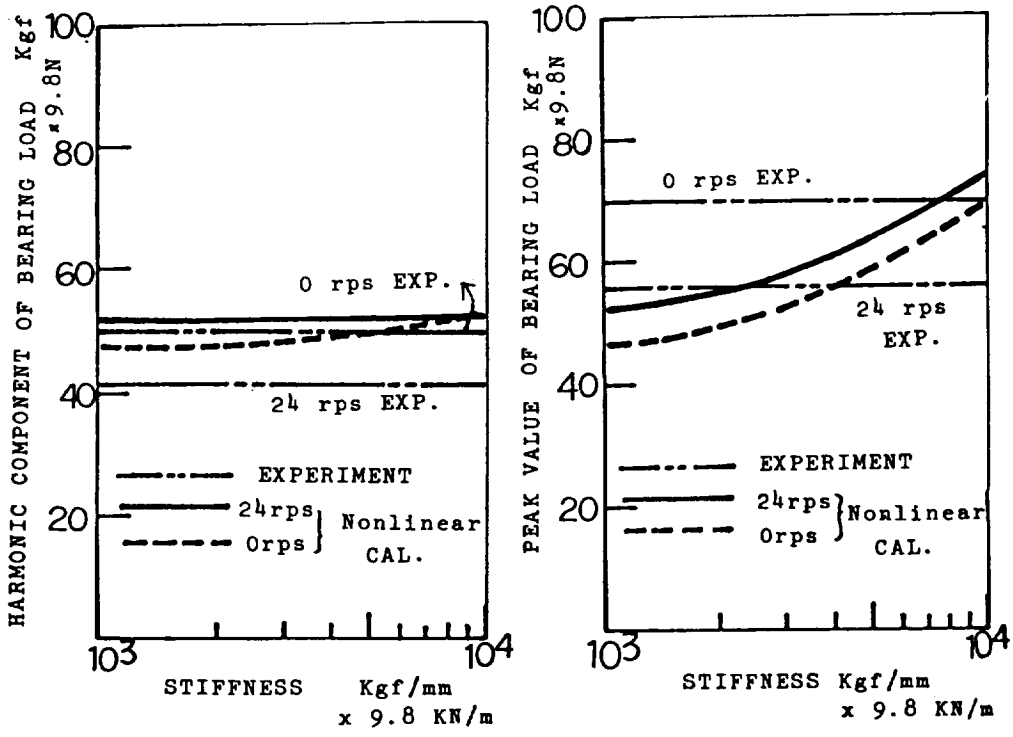

Figure 20. - Comparison of bearing dynamic load.

APPENDIX

Time History Response Analysis of Nonlinear Rotor-Bearing System by Quasi-Modal Technique

1. INTRODUCTION

In structure dynamics with many degrees of freedom of motion, time history response analysis involves two integration methods. One of them is direct integration and the other is modal. Generally speaking, the former is accurate, but not convenient for large structure systems because too much computational time is required. The latter is effective due to the great reduction of freedom of motion by the normal transformation, but its accuracy depends how many eigen vectors are introduced in the modal matrix. Each integration method inevitably contains its own advantagés and disadvantages.

These methods are also applied for non stationary rotor vibration analysis in rotor dynamics as well as in analyzing the gyroscopic effect and large damping force in bearings. The authors have already presented the special form of the orthogonality condition in rotor dynamics and the modal integration technique for analyzing non-stationary vibration of a rotor in a system with linearity or somewhat weak non-linearity.

In many cases, the modal technique is more convenient and powerful than the direct one. However, even the modal technique is not perfect and is inconvenient for time history response analysis in a rotor-bearing system with strong nonlinear boundary conditions.

However,in our experience it is very difficult to numerically simulate such a vibration mode -changing due to rubbing- by the modal integration technique,which guarantees only a linear system, and not a nonlinear one. The modal technique is limited to linear analysis and its forcible application to a nonlinear system is essentially unreasonable.

In this study a new method,which is exclusively applied for nonlinear analysis is developed on the basis of modal synthesis and the substructure method. A quasi-modal transformation is defined considering gyroscopic force and damping force for a general rotor system. The integration method is then introduced by the quasi-modal technique.

NOMENCLATURE

A,B : matrices after the quasi modal transformation
C : damping matrix
c^* : equivalent damping coefficient for the inner system
C_g : gyroscopic matrix
c_{g^*} : equivalent gyroscopic effect for the inner system
$F=[F_1,Q_2]^t$: external force
$F_1(t)$: external force acting upon the inner system
F_s : force on the quasi modal coordinate system
$i=\sqrt{-1}$: imaginary unit
K : stiffness matrix
k^* : equivalent stiffness for the inner system
M : mass matrix

$Q(z_2,\dot{z}_2,t)$: resistance force acting upon the boundary point
$S=[s_1,s_{2v},s_{2d}]^t$: state vector on the quasi-modal coordinate system
s_1 : weighting value corresponding to ϕ mode
$s_{2d}=z_2$: weighting value corresponding to δ mode,i.e.rotor displacement of the boundary point
$s_{2v}=\dot{z}_2$: weighting value corresponding to ξ mode,i.e.rotor velocity of the boundary point
t : time
$z=[z_1,z_2]^t$: rotor displacement vector in a complex form ($z=x+iy$)
z_1 : rotor displacement vector of the inner system
z_2 : rotor displacement of the boundary point
δ : deflection mode generated by the forced displacement
$\lambda=\alpha+iq$: complex eigenvalue
ξ : deflection mode generated by the forced velocity
Φ : matrix of the quasi-modal transformation
ϕ : eigen mode of the inner system
ψ : eigen mode of the entire system including the inner system and the boundary point
Ω : rotational speed
δ_{ij} : Dirac's function

2. QUASI-MODAL TRANSFORMATION

Equation of motion

This study deals with the rotor vibration in an entire system, including bearings and disks,as shown in Fig.1. The rotor displacement is measured on the coodinate system of O-XY$\overline{Z}$ which is fixed in the space. The complex form of the rotor displacement is denoted here by $z=x+iy$ for the displacements in the X-direction and Y-direction of x and y, respectively. The equation of motion of a rotor is written as:

$$M\ddot{z}+i\,\Omega C_g\dot{z}+K_f z+K_b\bar{z}+C_f\dot{z}+C_b\dot{\bar{z}}=F \qquad (1)$$

This equation represents the elliptical whirl motion of a rotor supported by general bearings with asymmetrical dynamic properties. In the case of the circular whirl motion due to symmetrical dynamic properties,
where

$$k_{xx}=k_{yy}\quad k_{xy}=-k_{yx}\quad C_{xx}=C_{yy}\quad C_{xy}=-C_{yx}\ ,$$

the equation of motion becomes little simpler, and can be written as:

$$M\ddot{z}+i\Omega\, C_g\dot{z}+Kz+C\dot{z}=F \qquad (2)$$

To simplify the description, the vibration of a vertically suspended rotor with symmetrical bearing dynamics is studied first and a new quasi-modal technique is presented. This technique is also extended to general rotor vibration including asymmetrical bearing dynamics, but the explanation is omitted in this paper.

Discrimination of boundary point and inner system

The cantilever type of rotor, as shown in Fig.2, is selected in order to clearly explain the concept of this new technique. In this rotor system, the left side is a fixed point which is clearly a boundary location. A bearing with non-

linearity is located on the right side of the rotor. It is assumed that the bearing dynamic properties are not constant.

This rotor system is a typical example of a system having one changing boundary condition. The right side is thus designated as a nonlinear boundary point, denoted by z_2. The rest of the rotor system is designated as a linear inner system, and its displacement vector is denoted by z_1.

A resistance force of Q_2 acts upon the boundary point, and an external force of F_1 is distributed on the inner system of the rotor.

The equation of motion (2) is rewritten, inserting displacements z_1 and z_2, as :

$$\begin{bmatrix} M_1 & 0 \\ 0 & M_2 \end{bmatrix}\begin{bmatrix} \ddot{z}_1 \\ \ddot{z}_2 \end{bmatrix} + i\Omega \begin{bmatrix} C_{g1} & 0 \\ 0 & C_{g2} \end{bmatrix}\begin{bmatrix} \dot{z}_1 \\ \dot{z}_2 \end{bmatrix} + \begin{bmatrix} K_{11} & K_{12} \\ K_{21} & K_{22} \end{bmatrix}\begin{bmatrix} z_1 \\ z_2 \end{bmatrix} + \begin{bmatrix} C_1 & 0 \\ 0 & C_2 \end{bmatrix}\begin{bmatrix} \dot{z}_1 \\ \dot{z}_2 \end{bmatrix} = \begin{bmatrix} F_1(t) \\ Q_2(z_2,\dot{z}_2,t) \end{bmatrix} \equiv F \qquad (3)$$

Where, subscripts 1 and 2 mean the inner system and the boundary point, respectively.

Transformation modes

An arbitrary vibration mode shape in the system with a changing boundary condition can be arranged by the synthesis of three kinds of special mode shapes, as shown in Fig.3. The quasi-modal transformation matrix thus consists of the three modes: ϕ , δ and ξ . The first two modes, ϕ and δ , are used in the conventional methods, called the substructure technique or modal synthesis. The third mode, ξ ,is introduced in this study for the first time and its necessity is emphasized.

ϕ mode

This is the complex eigen mode of the restricted system on the boundary point, as shown Fig.3(a). It is obtained by damped eigenvalue solving with respect to the M_1-C_{g1}-K_{11}-C_1 system.

The equation of motion of the inner system becomes

$$M_1\ddot{z}_1+i\Omega\, C_{g1}\dot{z}_1+K_{11}z_1+C_1\dot{z}_1=0 \qquad (4)$$

and the free vibration solution is assumed to be given by the following formula with the ϕ mode,

$$z= \phi\, e^{\lambda t} \qquad (5)$$

The orthogonality condition with respect to these eigen vectors is derived as:

$$\begin{bmatrix} \lambda_j \phi_j \\ \phi_j \end{bmatrix}^t \begin{bmatrix} -M_1 & 0 \\ 0 & K_{11} \end{bmatrix}\begin{bmatrix} \phi_k \lambda_k \\ \phi_k \end{bmatrix} = \delta_{jk}$$

$$\begin{bmatrix} \lambda_j \phi_j \\ \phi_j \end{bmatrix}^t \begin{bmatrix} i\Omega\, C_{g1}+C_1 & K_{11} \\ K_{11} & 0 \end{bmatrix}\begin{bmatrix} \phi_k \lambda_k \\ \phi_k \end{bmatrix} = \delta_{jk} \qquad (6)$$

δ mode

This is the deflection mode when the rotating shaft is subject to forced displacement on the boundary point,as shown in Fig.3(b). Under a load Q_2*, the

relationship between the shaft stiffness and the displacement is expressed as:

$$\begin{bmatrix} K_{11} & K_{12} \\ K_{21} & K_{22} \end{bmatrix} \begin{bmatrix} z_1 \\ z_2 \end{bmatrix} = \begin{bmatrix} 0 \\ Q_2^* \end{bmatrix} \tag{7}$$

where $Z_1 = \delta$ is the deflection mode
and $Z_2 = 1$ is the forced displacement on the boundary point. This load is equivalent to the shaft stiffness, when the inner system is viewed from the nonlinear boundary point, and is determined by the following relationship,

$$k^* = Q_2^* = K_{12}\,\delta + K_{22} \tag{8}$$

ξ mode

This is the deflection mode when the rotating shaft is subject to forced velocity on the nonlinear boundary point, as shown in Fig.3(c). This mode shape has not been used heretofore.

Under a load Q_2^*, which generates the forced velocity, the relationship including the gyroscopic force and the damping force up to the first-order differential equation of Eq.(3) becomes

$$\begin{bmatrix} i\,\Omega C_{g1}+C_1 & 0 \\ 0 & i\,\Omega C_{g2}+C_2 \end{bmatrix} \begin{bmatrix} \dot{z}_1 \\ \dot{z}_2 \end{bmatrix} + \begin{bmatrix} K_{11} & K_{12} \\ K_{21} & K_{22} \end{bmatrix} \begin{bmatrix} z_1 \\ z_2 \end{bmatrix} = \begin{bmatrix} 0 \\ Q_2^* \end{bmatrix} \tag{9}$$

Assuming the deflection of a nonlinear boundary point with

$$\dot{Z}_2 = 1 \qquad Z_2 = t, \tag{10}$$

the deflection mode shapes of the inner system with the form

$$\dot{Z}_1 = \delta \quad , \; Z_1 = \delta\, t + \xi \tag{11}$$

are determined by the following relationship

$$\xi = i\,\Omega\,\xi_g + \xi_c \tag{12}$$

where,

$$\xi_g = -K_{11}^{-1}\, C_{g1} \quad \delta = K_{11}^{-1}\, C_{g1} K_{11}^{-1}\, K_{12}$$

$$\xi_c = -K_{11}^{-1}\, C_1 \quad \delta = K_{11}^{-1}\, C_1\, K_{11}^{-1}\, K_{12}$$

Furthermore, this load Q_2^* is equal to the sum of equivalent gyroscopic effect c_g^* and equivalent damping coefficient c^*, when the inner system is viewed from the boundary point. The latter values are determined by the following formulas :

$$c_g^* = C_{g2} + \delta^t C_{g1}\, \delta \tag{13}$$

$$c^* = C_2 + \delta^t C_1\, \delta \tag{14}$$

Where,

$$Q_2^* = k^* t + i\,\Omega\, c_g^* + c^*$$

It is obvious in Eq.(12) that the ξ mode is generated by the gyroscopic force, reflecting the spin effect of the rotor, and by strong damping forces in the bearings. Thus these three modes must be considered in analyzing rotor dynamics. For ordinary structure dynamics, however, the third mode is not needed for the vibration analysis of nonrotating structures with negligible damping forces. This is why the conventional modal synthesis techniques applied to structure dynamics employ only the eigen mode ϕ of a restricted system and the deflection mode δ at a forced displacement. The new technique presented here for analyzing rotor dynamics is thus based upon a more general concept, and includes the usual substructure and modal synthesis techniques as well as the ξ mode.

Transformation of coordinate system

The quasi-normal transformation matrix is defined by analogy with the modal transformation, as follows :

$$\begin{bmatrix}\dot{z}\\ z\end{bmatrix} = \begin{bmatrix}\dot{z}_1\\ \dot{z}_2\\ z_1\\ z_2\end{bmatrix} = \begin{bmatrix}\phi\lambda & \delta & 0\\ 0 & 1 & 0\\ \phi & \xi & \delta\\ 0 & 0 & 1\end{bmatrix}\begin{bmatrix}s_1\\ \\ s_{2v}\\ s_{2d}\end{bmatrix} \equiv \Phi s \qquad (15)$$

The equation of motion of Eq.(2) is rewritten using a state equation :

$$\begin{bmatrix}-M & 0\\ 0 & K\end{bmatrix}\begin{bmatrix}\ddot{z}\\ \dot{z}\end{bmatrix} = \begin{bmatrix}i\Omega C_g+C & K\\ K & 0\end{bmatrix}\begin{bmatrix}\dot{z}\\ z\end{bmatrix} + \begin{bmatrix}-F\\ 0\end{bmatrix} \qquad (16)$$

Putting the transformation relationship of Eq.(15) into the state equation of Eq. (16), and premultiplying the transposed matrix of the transformation matrix Φ , a simple differential equation with respect to the quasi-modal coordinate of s vector is obtained as :

$$B\dot{s}=As-F_s \qquad (17)$$

where,

$$s=[s_1, s_{2v}, s_{2d}]^t$$

$$B=\begin{bmatrix}B_{11} & B_{12} & 0\\ B_{21} & B_{22} & 0\\ 0 & 0 & k^*\end{bmatrix} \quad A=\begin{bmatrix}A_{11} & 0 & 0\\ 0 & i\Omega c_g^*+c^* & k^*\\ 0 & k^* & 0\end{bmatrix} \quad F_s=\begin{bmatrix}(\phi\lambda)^t F_1\\ \delta^t F_1+Q_2\\ 0\end{bmatrix}$$

The structures of the transformed matrices B and A of Eq.(17) are shown in Fig.4. The matrices B_{11} and A_{11} contain zero elements in the off-diagonal part, because the eigen vectors of the linear inner system are orthogonal with each other, and these matrices become diagonal. The rest of B matrix, $B_{12}=B_{21}{}^t$ is equal to the nonzero elements because there is no orthogonality in the relationship between eigen vector ϕ and deflection modes δ and ξ . All off-diagonal elements of the coefficient matrices B and A are not zero, but many parts of them are. Consequently, this transformation can not give a theoretically perfect diagonalization of the transformed matrices, it does facilitate almost perfect diagonalization with non-zero elements at the edge of matrix B. This transformation technique is much closer to the modal one ; hence we call it the quasi-modal technique.

It should be noted that the almost perfect diagonalization with the non-zero

edge can not be accomplished without the ξ mode. That is why we introduce the ξ mode for this new quasi-modal technique.

In state equation (17) obtained by a quasi-modal transformation, the state vector s contains physical coordinates of $\dot{z}_2=s_{2v}$ and $z_2=s_{2d}$, corresponding to the velocity and displacement on the boundary point, respectively. And the resistance force Q_2 on the boundary point is also included in the force vector F_s without being reformed. These quantities related to the boundary point are maintained by the same description in the physical coordinate system. Therefore,the superposing operation is guaranteed after the quasi-normal transformation, as in the same manner as the FEM operation.

The degree of state equation (17) is equal to the degree of the modal transformation for the linear inner system plus twice the number of boundary points. Consequently the scale of the problem is greatly reduced,as compared with Eq.(3) or Eq.(17).

3. TIME HISTORY RESPONSE ANALYSIS

Hybrid Integration

The integration of the state equation (17) on the quasi-modal coordinate system gives the time history response under an external excitation $F_1(t)$.

The vector s_1 of the quasi-modal vector s indicates the weighted values corresponding to the eigen modes of the inner coordinate system. Thus, it can be said that the inner system is processed by the well known modal integration method.

On the other hand, the remaining elements of s_{2v} and s_{2d} in the quasi-modal vector s equal the physical coordinates with the relationship

$$z_2=s_{2d} \quad \dot{z}_2=s_{2v} \tag{18}$$

Thus, the boundary points are handle by physical quantities even in post-transformation, and are easily processed by the direct integration method.

Therefore, integration with respect to the quasi-modal coordinate s is equivalent to hybrid integration where modal and direction methods are mixed, as shown in Fig.5. The two conventinal methods have their own advantages and disadvantages, but the advantages of both methods are guaranteed in this new method. Thus the new technique is highly applicable to nonlinear vibration response analysis.

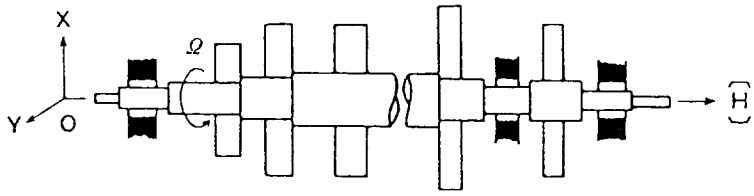

Figure 1. - Rotor-bearing system.

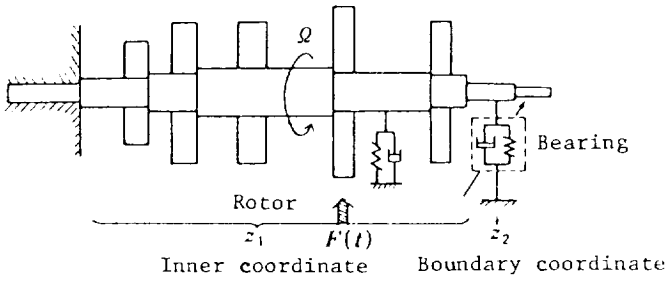

Figure 2. - Boundary point and inner system.

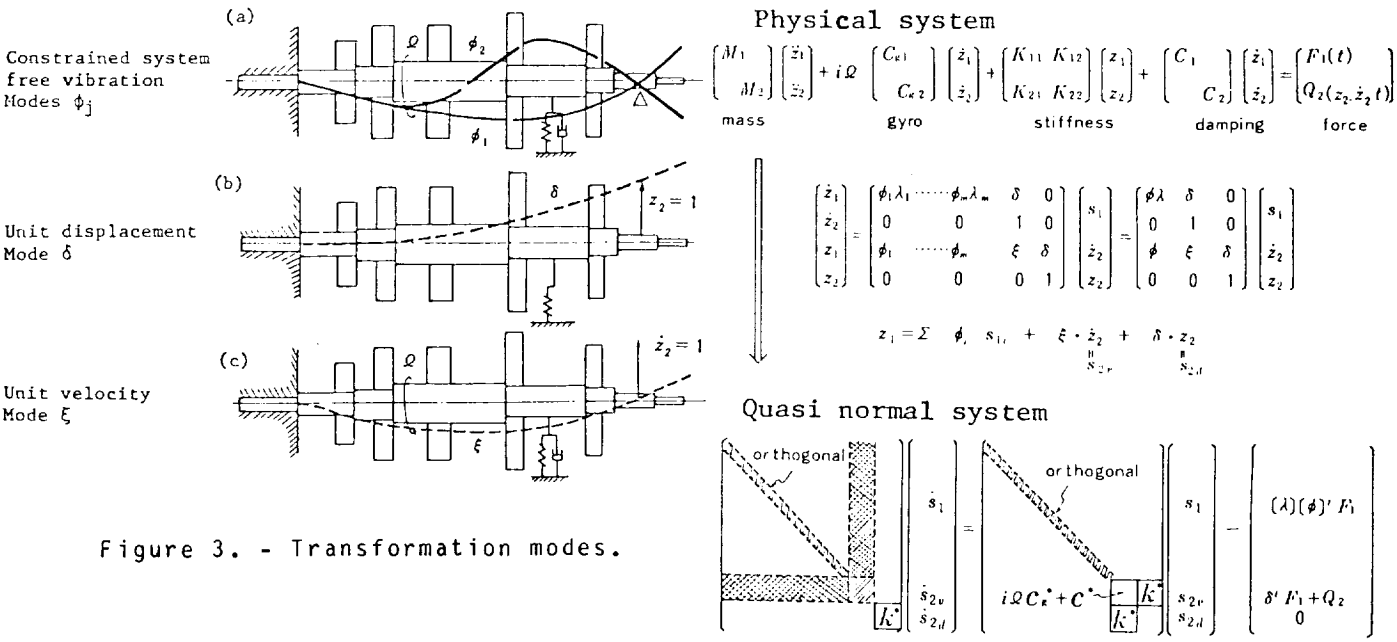

Figure 3. - Transformation modes.

Figure 4. - Quasi normal coordinate system.

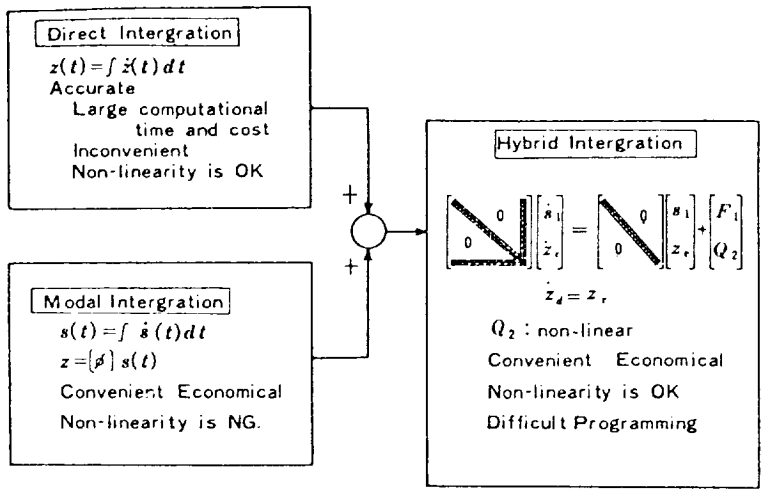

Figure 5. - Hybrid intergration.